Optik 151 (2017) 110–122

Contents lists available at ScienceDirect

Optik

journal homepage: www.elsevier.de/ijleo

Original research article

Visible light for communication, indoor positioning, and dimmable illumination: A system design based on overlapping pulse position modulation

Ata Chizari[a,b,*], Mohammad Vahid Jamali[a], Sajjad Abdollahramezani[c], Jawad A. Salehi[a], Akbar Dargahi[d]

[a] School of Electrical Engineering, Sharif University of Technology, P.O. Box 11365-11155, Tehran, Iran
[b] Biomedical Photonic Imaging Group, MIRA Institute for Biomedical Technology and Technical Medicine, University of Twente, P.O. Box 217, 7500 AE Enschede, The Netherlands
[c] School of Electrical and Computer Engineering, Georgia Institute of Technology, P.O. Box 30332-0360, 791 Atlantic Drive, NW, Atlanta, GA, USA
[d] School of Electrical Engineering, Shahid Beheshti University, P.O. Box 19839-69411, Tehran, Iran

ARTICLE INFO

Article history:
Received 21 March 2017
Received in revised form 13 July 2017
Accepted 1 August 2017

Keywords:
Visible light communications
Dimming support
System design
Indoor positioning
Overlapping pulse position modulation
Monte Carlo simulation
ALOHA
Channel sensing multiple access

ABSTRACT

In this paper, we design a dimming compatible visible light communication (VLC) system with asynchronous and optimum indoor positioning method in a standard office room in combination with asynchronous and optimum indoor positioning method according to illumination standards under channel constraints. We use overlapping pulse position modulation (OPPM) to support dimming control by changing the code weights. The system parameters such as a valid interval for dimming together with an upper bound for bit rate according to the channel delay spread are investigated. Moreover, considering the dispersive VLC channel and using Monte Carlo (MC) simulations, a method is proposed to determine the minimum code length in different dimming levels in order to achieve a valid bit error rate (BER). Then, the trellis coded modulation (TCM) is suggested to be applied to OPPM in order to take advantage of consequent coding gain which could be up to 3 dB. Finally, in order to enable asynchronously and with high throughput data transmission of LEDs for the purpose of indoor positioning, we propose using one-persistent carrier sense multiple access (CSMA) network protocol. Using received signal strength (RSS) based trilateration, the two dimensional positioning error of around 10 cm is verified by the simulation results.

1. Introduction

Nowadays, we are witness of a rapid growth in the communication service demands. It is expected that by 2020 an amount of 44 Zettabytes (44×10^{21}) of communication data will be on demand to be generated. The demand for wireless bandwidth capacity as predicted by Cisco (Cisco VNI.) shows a 10 times growth in mobile traffic till 2019. On the other hand, during the same years, the mobile carriers are predicted to be accelerated by 9% [1]. Moreover, the consumer electronics

* Corresponding author at: Biomedical Photonic Imaging Group, MIRA Institute for Biomedical Technology and Technical Medicine, University of Twente, P.O. Box 217, 7500 AE Enschede, The Netherlands.
E-mail address: a.chizari@utwente.nl (A. Chizari).

http://dx.doi.org/10.1016/j.ijleo.2017.08.003
0030-4026/

such as smart phones are expected to provide a high speed wireless communication in combination with the location based service (LBS). Meanwhile, the power consumption of such electronic devices which are approximated to be more than two times greater than the population of the world in numbers, should be optimized and be as low as possible. Therefore, the most important goal of the communication technologies is to save the energy in a large scale in order to enable the existence of future sustainable society [2].

Optical wireless communications has brought forward a potential framework for reaching secure, high-throughput, and cost-effective wireless communications in free-space [3,4], underwater [5–7], and multi-user indoor environments [8,9]. Specially saying that LiFi (light fidelity) technology, as a complementation of WiFi (wireless fidelity) is a smart solution to the aforementioned challenges. This disruptive technology which is a completed and enhanced form of visible light communication (VLC) can offer a complete package of illumination, high-speed data transmission in a network scale, and indoor positioning. To address the misconceptions regarding this technology, one can say that it is able to transmit hundreds of megabyte of data in a non-line-of-sight (NLOS) manner. The sunlight exposure to its receiver (generally a photodetector (PD)) can be considered as a direct current (DC) signal which is out of the range of the received signal. In the case that this exposure does not saturate the PD, the sunlight not only is not a problem for such systems, but also by employing the photovoltaic elements as the receiver, it is possible to harvest the energy to feed the receiver circuit. Additionally, the LiFi systems are able to provide dimming control by employing the appropriate modulation schemes [10,11].

To highlight the importance of this technology, let us mention some of its potential applications in our everyday life. LiFi technology can play an important role in the 5th generation of wireless communication networks (5G) as a coexistence with WiFi [12] providing full-duplex high-speed indoor access. It can enable light as a service (LaaS) in the market. It can contribute to road safety systems as the number of self-driving cars is rapidly growing. It will enable the asset tracking, for example, in a hospital to be aware of the situation of the wheelchairs and trolleys using visible light positioning techniques. The other application of the VLC positioning system would be in the museums to detect the location of a visitor and then to start playing the information media about the targeted asset [13]. It is over two decades that the research and investigation in the field of optical wireless communications (OWC) including VLC and specially LiFi is being done and a number of invaluable books has been published in this area [14–18] guiding the future researchers become familiar with the principles.

As mentioned earlier, VLC provides illumination in parallel to communication and positioning. Additionally, flicker mitigation and intensity control, also known as dimming control, are two noticeable requirements of such systems according to IEEE 802.15.7 task group [19]. Thus, utilizing robust modulation schemes that supply high data rate along with dimming control are imperative. Some dimming adaptable procedures for flicker-free high data rate VLC systems based on IEEE 802.15.17 standard are studied in [20]. The standard references in the channel model for typical indoor environments such as home and office are well investigated and proposed as IEEE 802.15.7r1 [21].

Among different kinds of modulation schemes, pulse position modulation (PPM) and its families are appropriate for intensity modulation with direct detection (IM/DD) communication systems such as VLC, since the chips within a code word can directly modulate a driver at the transmitter side. In recent years, many research interests have been attracted to overlapping PPM (OPPM) and its applications due to its high spectral efficiency and low bandwidth requirement. In [22] a method for supporting dimming by changing the amplitude of OPPM symbol pulses is proposed. Nevertheless, this may result in undesired chromaticity shift of the emitted light due to the characteristics of LEDs [23]. Researchers in [24] proposed multiple PPM (MPPM) to support dimming while transmitting data stream. They explored that MPPM outperforms variable PPM (VPPM) and variable on-off keying (VOOK), in terms of spectral efficiency and power requirement. Moreover, a solution to address the dimming control along with data transmission is suggested in [25] by changing OPPM code word weight.

This research is inspired by the need to design a VLC system with more spectral efficiency and less power requirement. In this paper, regarding dimming support by changing code weights of OPPM symbols, we consider a practical scenario within a standard room and design a system according to constraining parameters. To do so, we first determine an interval for dimming percentage in which the illumination standards are taken into account. Then, we calculate the maximum data rate for inter-symbol interference (ISI)-free transmission by simulating the dispersive channel response. Next, we propose a method to determine the maximum usable code length corresponding to a maximum bit error rate (BER) in the presence of different brightness percentages. Owing the fact that the modification in modulation and using coding schemes are essential to performance enhancement of VLC systems [26], we suggest applying trellis coded modulation (TCM) in order to take advantage of the corresponding coding gain which results in an improvement in the power requirement of OPPM. The validity of such application is depicted by simulation results. Finally, to complete the system design, we give a solution to channel access for different users for the purpose of unique code transmission. This enables the two dimensional indoor positioning within a hypothetical office room environment.

The rest of the paper is organized as follows. In Section 2, we briefly introduce the system and channel model. In Section 3, the system design according to OPPM scheme is investigated followed by the simulation results. Section 4, addresses the issue of channel access for the purpose of unique code transmissions together with an indoor positioning method compatible with the proposed system and finally, Section 5 concludes the paper.

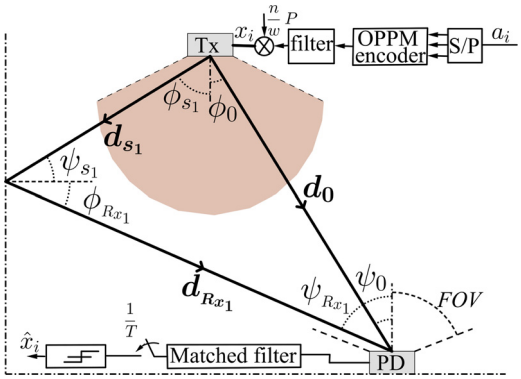

Fig. 1. System and channel model where Tx, and PD stand for driver and LED array, and photo-detector circuit, respectively.

2. System and channel model

2.1. System model

In this work, we assume the non-directed line-of-sight (LOS) VLC link in which transmitters and receivers have a wide range of transmission and field of view (*FOV*), respectively (see Fig. 1). Considering the baseband channel model for optical system, the photo-current generated by the receiver PD is given by;

$$Y(t) = RX(t) * h(t) + n(t), \tag{1}$$

where R denotes the PD responsivity (A/W), $X(t)$ is the transmitter optical power, * represents the convolution operator, and $n(t)$ is the receiver noise. This noise can be modeled as a signal dependent additive white Gaussian noise (AWGN) with double sided power spectral density of N_0 as [27];

$$N_0 = \sigma^2_{shot} + \sigma^2_{th} + \left(RP_{\mathrm{r}}^{(\mathrm{ISI})}\right)^2, \tag{2}$$

in which σ^2_{shot}, σ^2_{th}, and $P_r^{(\mathrm{ISI})}$ are shot noise variance, thermal noise variance, and the received power due to multipath reflection, respectively.[1] Moreover, the fact that $X(t)$ represents the instantaneous optical power, necessitates $X(t) > 0$ as well as $\lim_{T\to\infty} 1/2T \int_{-T}^{T} X(t)dt < P$, where P is the average optical power constraint of the transmitter LED [9].

2.2. Dimming support in OPPM

Consider an L-ary modulation scheme in the presence of AWGN and the maximum likelihood (ML) sequence detection, as well. The L non-negative symbols $\{x_1(t), x_2(t), \ldots, x_L(t)\}$ are sent with the bit rate R_b every $T = \log_2^L/R_b$ seconds. The average signal power is [28];

$$P = \frac{1}{L}\sum_{i=1}^{L} \langle x_i(t) \rangle, \tag{3}$$

where $\langle \cdot \rangle = \lim_{T\to\infty} 1/2T \int_{-T}^{T} x(t)dt$. Assuming high signal to noise ratio (SNR), the BER is dominated by two nearest signals and is given by $Q(d_{\min}/\sqrt{4N_0})$, where $d^2_{\min} = \min_{i\neq j} \int (x_i(t) - x_j(t))^2 dt$ is the minimum Euclidean distance between any pairs of valid symbols.

Looking at Fig. 1, the electrical bit sequence, a_i, is turned to parallel to be modulated by OPPM encoder. Then, after passing through filter and being normalized, the resulted modulated symbols, x_i, will be sent to block Tx, containing driver circuit and LED arrays. In the case of OPPM, the symbol interval T is divided to n chips and the temporal signal equation would be;

$$x(t) = \frac{P}{w}\sqrt{nT}\sum_{k=1}^{n-1} c_k \sqrt{\frac{n}{T}} p(t - k\frac{T}{n}), \tag{4}$$

[1] Note that based on comprehensive study of [27], the term σ^2_{shot} itself takes both incoming optical signal (desired and undesired interfering signals) and ambient background light into account.

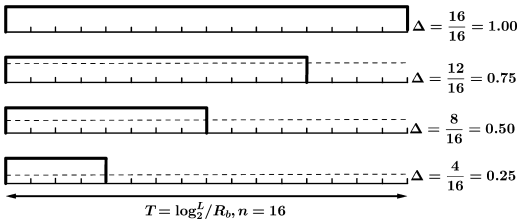

Fig. 2. Dimming control approach in OPPM, by changing the code weight. Dashed lines represent the transmitted optical power *P*.

where c_ks, for $k = 0, 1, \ldots, n-1$, are binary n-tuples of weight w, and $p(t)$ is a rectangular pulse with unit amplitude in the interval $[0, T/n]$. Note that $x(t)$ is always positive and fulfills the power constraint mentioned in Eq. (3). The w ones are restricted to be successive whereby the bandwidth requirement in this modulation scheme becomes smaller compared to that of L-PPM or MPPM. This advantage is offset by a reduction in the number of OPPM alphabet size. The number of symbols in OPPM is $L = n - w + 1$ and the bandwidth requirement is given by;

$$B^{(\mathrm{OPPM})} = \frac{n/w}{\log_2^L / R_\mathrm{b}}. \tag{5}$$

Hence, the maximum achievable bit rate and the spectral efficiency can be respectively calculated as follows [28];

$$\begin{aligned} R_b &< B^{(\mathrm{OPPM})} \Delta \log_2^L, \\ SE &= \frac{1}{\Delta} \log_2^L, \end{aligned} \tag{6}$$

where $\Delta = w/n$ denotes the duty cycle. Now, in contemplation of controlling the intensity of incident light, one can change the weight of symbols, w, while remaining the number of chips, n, unchanged [25]. This technique is shown in Fig. 2 in which four dimming levels are illustrated. Obviously, in the cases of $\Delta = 1$ and 0, i.e., full brightness and full darkness, respectively, no data could be transmitted. We also refer to $100\sqrt{\Delta}\%$ as the perceived brightness percentage in that it is more compatible with the nonlinear response of the human eye to the linear changes in the intensity of visible light [20].

2.3. Channel model

The SNR value can be expressed as [9];

$$\mathrm{SNR} = \frac{\left(RP_\mathrm{r}^{(\mathrm{LOS})}\right)^2}{N_0 B^{(\mathrm{OPPM})}} = \frac{\left(RH^{(\mathrm{LOS})}(0)P_t\right)^2}{N_0 B^{(\mathrm{OPPM})}}, \tag{7}$$

where t and r stand for transmitted and received terms, respectively. $H^{(\mathrm{LOS})}(0)$ is the portion of channel DC gain arising from the LOS link which is given by [17];

$$H^{(\mathrm{LOS})}(0) = \begin{cases} A_r \dfrac{m+1}{2\pi d_0^2} \cos^m(\phi_0) T_s(\psi_0) & \\ \quad \times g(\psi_0) \cos(\psi_0), & 0 \le \psi_0 \le FOV \\ 0, & \text{Otherwise} \end{cases} \tag{8}$$

where A_r denotes the PD active area, m is Lambert's mode number of a radiation lobe, $-1/\log_2(\cos(\phi_{1/2}))$ in which $\phi_{1/2}$ represents the semi-angle at half power of an LED, $T_s(\cdot)$ and $g(\cdot)$ represent the optical bandpass filter transmission and non-imaging concentrator gain of the receiver, and ϕ_0 and ψ_0 are the angle of irradiance and incidence, respectively, as shown in Fig. 1.

The impulse response in the time domain is defined as $H^{(\mathrm{LOS})}(0)\delta(t - d_0/c)$, where $\delta(\cdot)$ represents Dirac delta function and c is the light velocity. Thus, the received optical power from LOS path is $P_r^{(\mathrm{LOS})} = H^{(\mathrm{LOS})}(0)P_t$. For the sake of simplicity, we

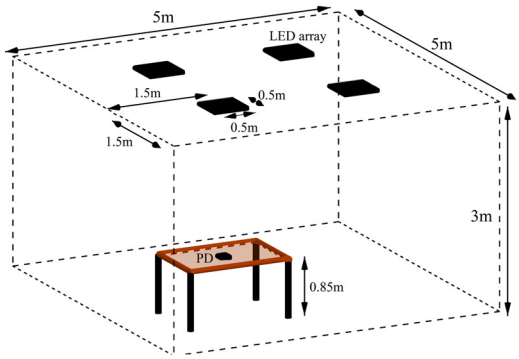

Fig. 3. The hypothetical office room containing four Landmarks and a PD.

Table 1
System parameters.

Transmitter side	
Number of LED fixtures	4
LED fixture area	$0.5 \times 0.5\,m^2$
Number of LEDs within a fixture	324
LED spacing in a fixture	2.8 cm
LED power	63 mW
Semi-angle at half power ($\phi_{1/2}$)	70°
Center luminous intensity	9.5 cd
Receiver side (photo-detector)	
Position	(1, 1, 0.85) m
Area (A_r)	$1\,cm^2$
Field of view (FOV)	60°
Ambient light current	27 mA
Responsivity (R)	0.28 A/W

consider only the first reflection which is more dominant than the higher order reflections. So, the NLOS channel response is given by;

$$\begin{aligned} h^l(t,S,R_x) &= \sum_{j=1}^{\Re} \frac{(m+1)\rho_j A_r \Delta A}{2\pi d_{s_j}^2 d_{R_{x_j}}^2} \cos^m(\phi_{s_j}) \cos(\psi_{s_j}) T_s(\psi_{R_{x_j}}) \\ &\quad \times g(\psi_{R_{x_j}}) \cos(\phi_{R_{x_j}}) \cos(\psi_{R_{x_j}}) \delta\left(t - \frac{d_{s_j} + d_{R_{x_j}}}{c}\right) \\ &= H^{(NLOS)}(0)\delta\left(t - \frac{d_{s_j} + d_{R_{x_j}}}{c}\right), \end{aligned} \tag{9}$$

where S represents the reflectors' surface (consists of four walls in the hypothetical room), ρ_j is the reflection index of the jth reflector, ΔA is the element area of reflectors, and $\Re$ denotes the number of reflectors, i.e., walls.

3. System design and simulation results

In this section, we design a system according to what was introduced in Section 2. With respect to designing a dimming compatible indoor VLC system assuming practical situation of an office room, we contemplate a $5 \times 5 \times 3\,m^3$ room having four fixtures of LEDs as well as a table of height 0.85 m under one of the fixtures with a PD on its center. This scenario is shown in Fig. 3. Furthermore, the specification of transmitters and receivers utilized in simulations is summarized in Table 1 where some of LED and PD parameters are extracted from [29].

3.1. Illumination standards

The main goal of VLC systems is to provide illumination as well as communication. Therefore, in an office environment the illumination generated by LEDs must satisfy illumination standards. The horizontal illuminance resulted by OPPM modulation with dimming support on a surface is given by;

$$E_h = \frac{w}{n} \frac{I_0 \cos^m(\phi_0 right) \cos(\psi_0)}{d_0^2}, \tag{10}$$

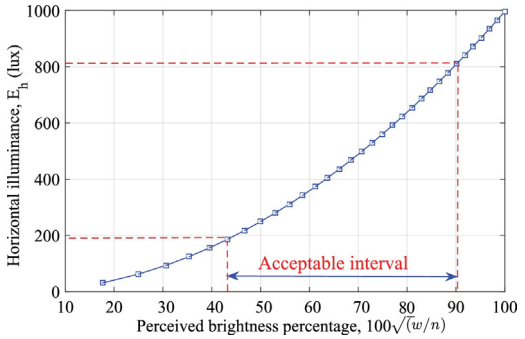

Fig. 4. Received illuminance at the location of PD versus perceived brightness percentage.

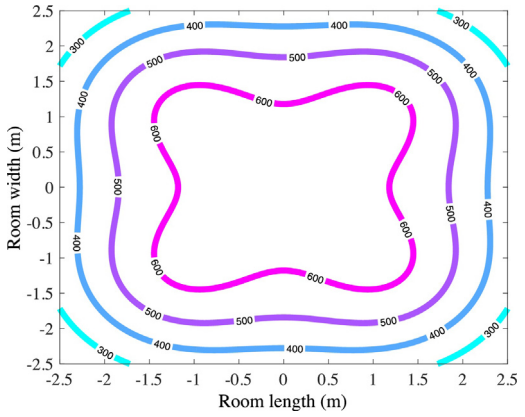

Fig. 5. Distribution of brightness within the room at 80% of perceived brightness.

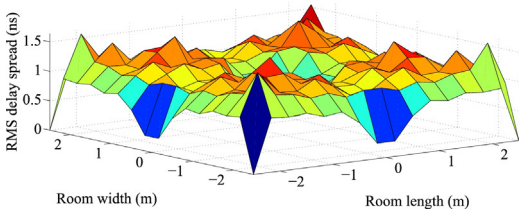

Fig. 6. Distribution of RMS delay spread within the given room.

where I_0 represents the center luminous intensity of LEDs. According to [29], the standard illuminance level within an office room is between 200 and 800 lux. The variation of horizontal illuminance in terms of different dimming levels in the hypothetical room is depicted in Fig. 4. Note that this figure is obtained at the position of PD shown in Fig. 3. Hence, concerning the illumination budget, a range of 44 to 90 percent of perceived brightness would be achievable. Moreover, the distribution of illuminance within the room at 80% of perceived brightness is illustrated in Fig. 5. It is worth to be mentioned that the acquired interval for dimming, fulfills the standard around the table on which the PD is installed.

3.2. Maximum achievable bit rate

The bit rate in VLC systems is affected by multipath reflections. An established criterion for defining its upper bound is root mean square (RMS) of delay spread which is given by [17];

$$D = \sqrt{\frac{\int (t-\mu)^2 h^2(t)dt}{\int h^2(t)dt}}, \tag{11}$$

where $\mu = \int th^2(t)dt / \int h^2(t)dt$ is the mean delay resulted by NLOS paths and $h(t)$ is the dispersive channel impulse response. Therefore, to guarantee an ISI-free transmission, the maximum bit rate should be less than $1/(10D)$. The delay spread parameter depends on room dimensions, location of transceivers (transmitters and receivers), and also the *FOV* of PD. Fig. 6 depicts

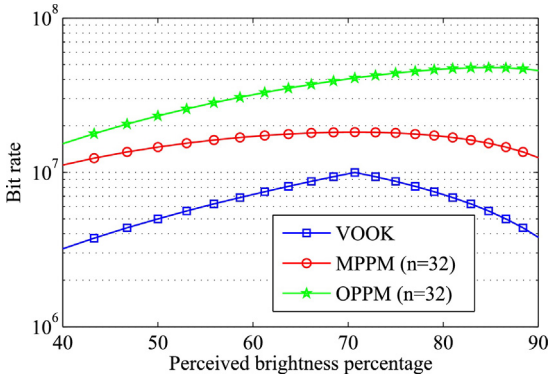

Fig. 7. Maximum bit rate theoretically achievable in terms of allowable dimming interval.

$d_c = 2$ $(C_1, C_2, C_3, C_4, C_5, C_6, C_7, C_8, C_9, C_{10}, C_{11}, C_{12}, C_{13}, C_{14}, C_{15}, C_{16})$
$d_c = 4$ $(C_1, C_3, C_5, C_7, C_9, C_{11}, C_{13}, C_{15})$ $(C_2, C_4, C_6, C_8, C_{10}, C_{12}, C_{14}, C_{16})$
$d_c = 8$ (C_1, C_5, C_9, C_{13}) $(C_3, C_7, C_{11}, C_{15})$ $(C_2, C_6, C_{10}, C_{14})$ $(C_4, C_8, C_{12}, C_{16})$
$d_c = 16$ (C_1, C_9) (C_5, C_{13}) $(C_3, C_{11})(C_7, C_{15})$ $(C_2, C_{10})(C_6, C_{14})$ (C_4, C_{12}) (C_8, C_{16})

Fig. 8. 1, 2, 4, and 8-states set partitioning.

the distribution of RMS delay spread within the room. This parameter at the position of PD in the hypothetical room is obtained as 1.28 ns. Hence, the bit rate would be upper bounded by 78 Mbps. On the other hand, the maximum bit rate theoretically achievable for different modulation schemes, namely VOOK, MPPM, and OPPM, versus 44 to 90 percent of perceived brightness is illustrated in Fig. 7. The OPPM modulation scheme not only gives the highest bit rate (e.g., up to 50 Mbps compared to MPPM and VOOK [24] which give 20 Mbps and 7 Mbps, respectively, at 80% of perceived brightness), but also referring Eq. (6) the peak value of OPPM bit rate, which is 50 Mbps, is less than the upper bound achieved due to channel constraint, namely 78 Mbps. Note that the modulation bandwidth of LEDs is supposed to be about 20 MHz, because although the bandwidth offered by off-the-shelf phosphor-based LEDs is about 2 MHz, it could be improved to 20 MHz by installing a blue filter on PD in order to remove the yellowish component of the received light.

3.3. Trellis coded OPPM

It is widely known that TCM improves system performance without increasing the required bandwidth. Since OPPM symbols have relatively low duty cycle and equal energy, if the duty cycle Δ stands fix, then doubling the number of symbols L leads the bandwidth to remain constant [30]. For this reason, the number of chips of the eventuated TCM 2L-OPPM can be calculated as $n_c = (2L-1)/(1-\Delta)$ and the equivalent weight would be $w_c = \Delta n_c$. However, by applying TCM to OPPM the minimum hamming distance between symbols decreases which causes to a growth in the probability of error. Fortunately, the arisen coding gain via set partitioning retrieves the performance degradation of reduced minimum hamming distance. Fig. 8 outlines the set partitioning of the OPPM with $n = 16$. The bandwidth requirement of the TCM 2L-OPPM is the same as uncoded OPPM and can be calculated using Eq. (5), yet the required average power could be lessened as is described in the following.

Considering the minimum hamming distance as $d = P/w\sqrt{dnT} = 2$ for uncoded OPPM [28], the BER would be;

$$BER = Q\left(\frac{P\sqrt{dnT}}{2w\sqrt{N_0}}\right). \tag{12}$$

By solving the last equation for P, the average required optical power of the uncoded OPPM can be extracted as;

$$P_{uc}^{(\mathrm{OPPM})} = 2w\sqrt{\frac{N_0}{2nT}}Q^{-1}(BER). \tag{13}$$

Nevertheless, for TCM 2L-OPPM we have;

$$P_{\mathrm{TCM}}^{(2L-\mathrm{OPPM})} = 2\Delta w\sqrt{\frac{N_0}{d_c\frac{2L-1}{1-\Delta}T}}Q^{-1}(BER), \tag{14}$$

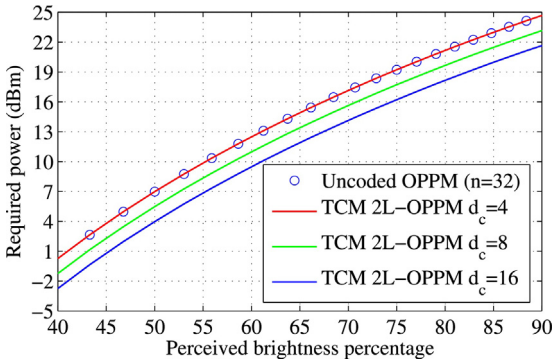

Fig. 9. Average optical power requirement of OPPM ($BER = 10^{-6}$) in terms of allowable dimming interval at the location of PD within the hypothetical room.

where d_c is the minimum hamming distance between TCM 2L-OPPM symbols. Therefore, the consequent coding gain, in terms of dB, is given by;

$$\frac{P_{uc}^{(\mathrm{OPPM})}}{P_{\mathrm{TCM}}^{(2L-\mathrm{OPPM})}} = 10\log_{10}\left(\frac{L-1}{2L-1}\sqrt{\frac{d_c}{2}\frac{2L-1}{L-1}}\right) \approx 10\log_{10}\left(\sqrt{\frac{d_c}{4}}\right). \tag{15}$$

For the sake of achieving the coding gain, d_c needs to be greater than four, e.g., examine 9-OPPM with $w = 8$. A coding gain equal to 1.2 dB is attainable by choosing a 4-state set partitioning of the TCM 18-OPPM with $w_c = 17$ along with the same bandwidth requirement. Altogether, the superiority of trellis coded OPPM over uncoded OPPM is depicted in Fig. 9, in which the power requirement to achieve a BER of 10^{-6} through the given room is plotted in terms of the qualified dimming interval. As mentioned in Eq. (15), although the required power for uncoded and TCM 2L-OPPM with $d_c = 4$ are the same, increasing d_c to 8 and 16 leads to a reduction of 2.55 dB and 3 dB in power requirement, respectively with the same bit rate.

3.4. Minimum required code length

As the third part of system design considered in this paper, we need to analyze the system from the BER viewpoint. Referring Eq. (12) and assuming $d = 2$ for uncoded OPPM and also $T = \log_2^L/R_b$, one can write [28];

$$BER = Q\left(\frac{P}{w}\sqrt{\frac{n\log_2^L}{2R_bN_0}}\right). \tag{16}$$

In this equation, n is the code length which needs to be chosen in order to achieve an acceptable bit error probability. To do so, the maximum BER of 3×10^{-3} as a threshold for forward error correction (FEC) is supposed. The parameter N_0 in Eq. (16) contains the contributions of shot noise, thermal noise, and multipath reflections. Therefore, we simulate the system shown in Fig. 1 in two steps.

Step I: A transmitter containing OPPM encoder sends modulated symbols through the channel in which the noise is considered to be AWGN. At the receiver side the temporal data streams after passing through a filter which is matched with the transmitted pulse shape, $p(t)$, and being sampled with rate $1/T$, are detected using a hard decision block. Finally, the bit error probability is calculated using MC simulation, in terms of different SNRs. This procedure is repeated for 4 dimming levels, namely 35, 50, 75, and 86% which are illustrated in Fig. 10, respectively. Furthermore, in each dimming level, such simulation is done with 5 different code lengths.
Step II: In this step, to consider channel and receiver constraints, including the effects of multipath reflectors, signal dependent shot noise, and thermal noise [27], the ratio of received optical power to sum of noise contributions is simulated within the hypothetical room to determine the channel SNR according to Eq. (7).

Fig. 11 depicts the SNR in terms of a range of dimming levels. As a consequence, to choose an appropriate code length for a specific dimming level, one can extract the amount of channel SNR in order to determine the probability of error from the corresponding curve (Fig. 10). For instance, for 50% of dimming, the channel SNR using Fig. 11 would be −0.5 dB. Then, regarding Fig. 10b the code lengths 32, 64, and 128 have BER values less than the predetermined BER threshold, i.e., 3×10^{-3}. Thus, the minimum code length of 32 can be used in this dimming level. Table 2 summarizes minimum code length appropriate for different levels of dimming.

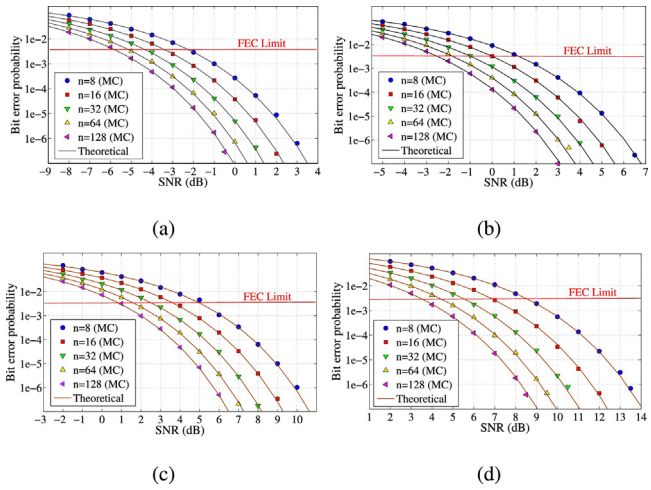

Fig. 10. Bit error probability of OPPM versus SNR for (a) 35%, (b) 50%, (c) 75%, and (d) 86% of perceived brightness percentages.

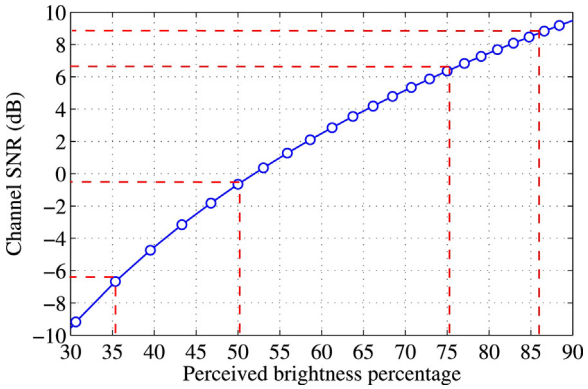

Fig. 11. Simulation of channel SNR within the hypothetical room at the location of PD for different levels of perceived brightness percentages.

Table 2
Minimum acceptable code length for various perceived brightness percentages.

Dimming level (%)	Channel SNR (dB)	Minimum acceptable n
35	−6.2	128
50	−0.5	32
75	6.5	8
86	8.5	8

4. Indoor positioning and multiple access considerations

One of the important applications of VLC systems is localization in indoor environments such as malls for the purpose of advertisements. There have been several methods introduced for indoor positioning such as triangulation, scene analysis, and proximity. Offering the best accuracy, we focus on triangulation method for defining the position of PD. This method requires at least three reference points to give an estimate of the receiver's location. This means that at least three LED transmitters around the detector should send their unique code to the receiver. Therefore, there is a need to investigate an efficient media access control (MAC) protocol for the VLC positioning system.

4.1. Channel access protocols for transmitters

In order to enable the transmitters send their identification data (in the present work, in the form of an OPPM signal) to the receiver, one can use the well-known ALOHA (Additive Links On-line Hawaii Area) random access network protocol. In a basic ALOHA technique which is called pure ALOHA or un-slotted ALOHA, the transmitters (nodes) within a dedicated medium (free space channel in this work) compete with each other to be able to successfully send their data. The channel

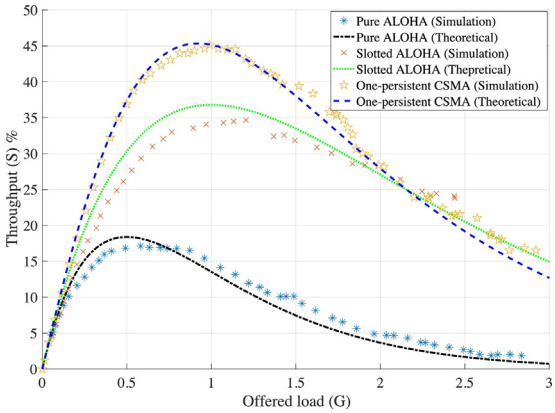

Fig. 12. A simulation of channel throughput percentage in terms of offered traffic for pure ALOHA, slotted ALOHA, and one-persistent CSMA.

throughput percentage in this protocol is defined as the number of successfully transmitted packets per total transmission time [31] and can be written as;

$$S = 100Ge^{-2G}, \tag{17}$$

where G is the offered traffic, defined by the time for total number of offered traffics (packets) per total transmission time. The throughput in pure ALOHA can roughly reach 18 percent where $G = 0.5$. As an alternation to pure ALOHA, the slotted ALOHA has been introduced in which the nodes are bound to send their packets in the appropriate times forming slots in a frame. In this scheme, the partial collisions are aborted and the collision can take place as full collision. As a consequence, the throughput can be rewritten as;

$$S = 100Ge^{-G}, \tag{18}$$

where the maximum throughput reaches 36 percent at $G = 1$. Note that in the slotted ALOHA, transmitters should be synchronized to each other in order for setting a reference clock as a time source. To solve this issue and also to reach a higher throughput, we suggest to equip the system with channel access techniques such as one-persistent carrier sensing multiple access (CSMA) technique. In this scenario, each transmitter ready for sending data, first listens to the channel, in case it is free, it sends the data and waits for its acknowledgment. If the channel is busy, it keeps sensing the channel and as soon as it is free, the node transmits the data immediately and then waits for the acknowledgment. Therefore, not only there is no need to the nodes to be synchronized to each other, but also we can see an improvement in the channel throughput. This parameter in this case can be defined as [32];

$$S = 100Ge^{-G(1+2\alpha)}\frac{1+G+\alpha G(1+G(1+\alpha/2))}{G(1+2\alpha)-(1-e^{-\alpha G})+(1+\alpha G)e^{-G(1+\alpha)}}, \tag{19}$$

where α is the fraction of propagation delay to the packet duration. Fig. 12, compares three aforementioned protocols where we can conclude that one-persistent CSMA outperforms pure and slotted ALOHA, with a peak of 45 percent at $G = 1$. The simulation results with a good agreement with theories also verify the superiority of this channel access technique.

4.2. Positioning method

According to what mentioned earlier, offering high accuracy, indoor positioning is one of the key features of VLC system. To complete our system design, let us focus on an accurate localization scheme, namely, received signal strength (RSS) based trilateration which is able to estimate the two dimensional location of the receiver device.

Referring Eq. (8) and considering $P_r^{(LOS)} = H^{(LOS)}(0)P_t$ one can write;

$$d = \sqrt{\frac{(m+1)A\cos^m(\phi)T_s(\psi)g(\psi)\cos(\psi)P_t}{2\pi P_r}}, \tag{20}$$

where $m = 1$ and d is the direct distance from each transmitter to the PD. We suppose that the transmitters and receiver depicted in Fig. 3 are located in the same normal axis, i.e. ($\psi = \phi$). Taking a look at Fig. 1, we can write $cos(\phi) = Z/d$ and $d_{xy} = \sqrt{d^2 - Z^2}$ where Z is the vertical distance from ceiling to the surface of the table which is supposed to be 2.15 m in

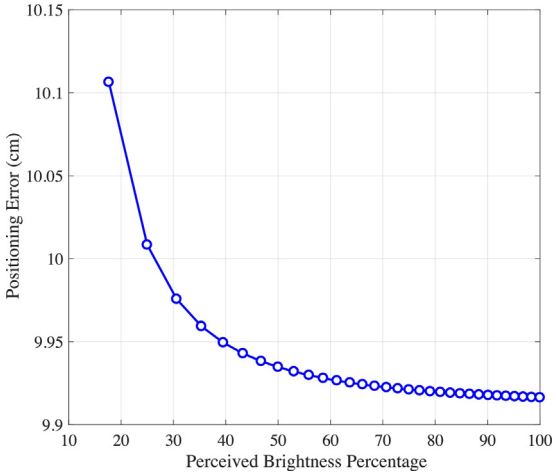

Fig. 13. Two dimensional positioning error at the location of the PD in terms of the perceived brightness percentage ($100\sqrt{w/n}$) when $n = 32$.

this work and d_{xy} is defined as the horizontal distance between a transmitter and the receiver. Therefore, the last equation can be simplified as;

$$d_{xy} = \sqrt{Z\left(\sqrt{\frac{AGRP_{\mathrm{t}}}{\pi P_{\mathrm{r}_i}}} - Z\right)}, \qquad i \in \{1, 2, 3, 4\}, \tag{21}$$

where $G = g(\psi)T_s(\psi)$ is a constant value related to the concentrator installed on the detector and $P_{\mathrm{r}_i} = R\left(P_{\mathrm{r}_i}^{(LOS)} + P_{\mathrm{r}_i}^{(ISI)}\right) + \sigma_{\mathrm{shot}}^2 + \sigma_{\mathrm{th}}^2$ is the total electrical signal at the receiver side. Note that in order to better simulate it, we consider that $R = 1$ which is of course an ideal assumption.

Now, if the unique codes from three transmitters are received by the detector, it is able to measure the receiving optical powers and makes an estimation of its two dimensional location (x,y). This method is called RSS based trilateration which is described in detail in [33]. Suppose that locations of transmitters (x_1,y_1), (x_2,y_2), and (x_3,y_3) are known to the receiver, by measuring the received powers, it can calculate its two dimensional distance with respect to each transmitter as $d_{x_1y_1}$, $d_{x_2y_2}$, and $d_{x_3y_3}$ and write;

$$\begin{aligned} (x_1 - x)^2 + (y_1 - y)^2 &= d_{x_1y_1}^2, \\ (x_2 - x)^2 + (y_2 - y)^2 &= d_{x_2y_2}^2, \\ (x_3 - x)^2 + (y_3 - y)^2 &= d_{x_3y_3}^2. \end{aligned} \tag{22}$$

By subtracting the second and third equations to the first one, we can remove the non-linear part and write;

$$\mathbf{X} = \mathbf{A}^{-1}\mathbf{B}, \tag{23}$$

where

$$\mathbf{X} = \begin{bmatrix} x & y \end{bmatrix}^T, \tag{24}$$

$$\mathbf{X} = \begin{bmatrix} x & y \end{bmatrix}^T, \tag{25}$$

$$\mathbf{B} = \frac{1}{2}\begin{bmatrix} d_{x_1y_1}^2 - d_{x_2y_2}^2 + (x_2^2 + y_2^2) - (x_1^2 + y_1^2) \\ d_{x_1y_1}^2 - d_{x_3y_3}^2 + (x_3^2 + y_3^2) - (x_1^2 + y_1^2) \end{bmatrix}. \tag{26}$$

Fig. 13 presents the two dimensional positioning error at the location of the receiver versus a range of perceived brightness percentages. The simulation has been run for $n = 32$, the number of chips described earlier. The error is calculated as $e = \sqrt{(x_m - x_r)^2 + (y_m - y_r)^2}$ where m and r stand for measured and real. The error value is around 10 cm which is due to the contribution of shot noise, thermal noise and the first order reflection of the walls. It can also be inferred that at the lower dimming levels, the less received power leads to a higher amount of positioning error. In order to improve the system performance as of the estimation error, one can investigate an extended Kalman filter (EKF) according to the initial knowledge of the expected receiver power [34]. This can be of an attractive topic for the future work as a combination of RSS and EKF.

5. Conclusion

In the present work, we investigated the design of a VLC system which supports dimmable illumination, high-speed communication, and asynchronous and accurate two dimensional positioning. We exploited OPPM due to its less power requirement in comparison to MPPM. The dimming control was addressed by changing the code weights while remaining the code lengths unchanged. At first, the dimming interval of 44 to 90 percent was determined according to illumination standards in a hypothetical office room. Then, an upper bound of 78 Mbps for ISI-free transmission was obtained via simulation of dispersive channel. Moreover, TCM was suggested to be applied to OPPM in order to take advantage of about 3 dB coding gain. The minimum code length that achieves a minimum BER for different dimming levels was obtained via MC simulation. Finally, the one-persistent CSMA MAC protocol was suggested to be applied to the system in order to enable two dimensional positioning with an optimum channel access for unique code transmission. The simulation results showed that the positioning error remains around 10 cm with the range of dimming levels.

Acknowledgments

Portion of this work was presented at the conference CSNDSP in 2016, paper “Designing A Dimmable OPPM-Based VLC System Under Channel Constraints” [35]. The authors would like to thank Professor Seyed Mohammad Sajad Sadough and Professor Seyed Ali Ghorashi for their constructive help. This research did not receive any specific grant from funding agencies in the public, commercial, or not-for-profit sectors.

References

[1] N. Chi, H. Haas, M. Kavehrad, T.D. Little, Visible light communications: demand factors, benefits and opportunities, IEEE Wireless Commun. 22 (2) (2015) 5–7, http://dx.doi.org/10.1109/MWC.2015.7096278 (guest editorial).
[2] M. Collotta, G. Pau, An innovative approach for forecasting of energy requirements to improve a smart home management system based on BLE, IEEE Trans. Green Commun. Netw. (2017) 112–120, http://dx.doi.org/10.1109/TGCN.2017.2671407.
[3] X. Zhu, J.M. Kahn, Free-space optical communication through atmospheric turbulence channels, IEEE Trans. Commun. 50 (8) (2002) 1293–1300, http://dx.doi.org/10.1109/TCOMM.2002.800829.
[4] H. Willebrand, B.S. Ghuman, Free Space Optics: Enabling Optical Connectivity in Today’s Networks, SAMS Publishing, 2002.
[5] M.V. Jamali, F. Akhoundi, J.A. Salehi, Performance characterization of relay-assisted wireless optical CDMA networks in turbulent underwater channel, IEEE Trans. Wireless Commun. 15 (6) (2016) 4104–4116, http://dx.doi.org/10.1109/TWC.2016.2533616.
[6] M.V. Jamali, J.A. Salehi, F. Akhoundi, Performance studies of underwater wireless optical communication systems with spatial diversity: MIMO scheme, IEEE Trans. Commun. 65 (3) (2017) 1176–1192, http://dx.doi.org/10.1109/TCOMM.2016.2642943.
[7] M.V. Jamali, A. Chizari, J.A. Salehi, Performance analysis of multi-hop underwater wireless optical communication systems, IEEE Photonics Technol. Lett. 29 (5) (2017) 462–465, http://dx.doi.org/10.1109/LPT.2017.2657228.
[8] H. Ma, L. Lampe, S. Hranilovic, Coordinated broadcasting for multiuser indoor visible light communication systems, IEEE Trans. Commun. 63 (9) (2015) 3313–3324, http://dx.doi.org/10.1109/TCOMM.2015.2452254.
[9] J.M. Kahn, J.R. Barry, Wireless infrared communications, Proc. IEEE 85 (2) (1997) 265–298, http://dx.doi.org/10.1109/5.554222.
[10] H. Haas, LiFi: conceptions, misconceptions and opportunities, in: Photonics Conference (IPC), 2016 IEEE, IEEE, 2016, pp. 680–681, http://dx.doi.org/10.1109/IPCon.2016.7831279.
[11] H. Haas, A light-connected world, Phys. World 29 (8) (2016) 30, http://dx.doi.org/10.1088/2058-7058/29/8/33.
[12] M. Ayyash, H. Elgala, A. Khreishah, V. Jungnickel, T. Little, S. Shao, M. Rahaim, D. Schulz, J. Hilt, R. Freund, Coexistence of WiFi and LiFi toward 5G: concepts, opportunities, and challenges, IEEE Commun. Mag. 54 (2) (2016) 64–71, http://dx.doi.org/10.1109/MCOM.2016.7402263.
[13] J. Armstrong, Y. Sekercioglu, A. Neild, Visible light positioning: a roadmap for international standardization, IEEE Commun. Mag. 51 (12) (2013) 68–73, http://dx.doi.org/10.1109/MCOM.2013.6685759.
[14] S. Dimitrov, H. Haas, Principles of LED Light Communications: Towards Networked Li-Fi, Cambridge University Press, 2015.
[15] S. Arnon, Visible Light Communication, Cambridge University Press, 2015.
[16] M. Uysal, C. Capsoni, Z. Ghassemlooy, A. Boucouvalas, E. Udvary, Optical Wireless Communications: An Emerging Technology, Springer, 2016.
[17] Z. Ghassemlooy, W. Popoola, S. Rajbhandari, Optical Wireless Communications: System and Channel Modelling With Matlab®, CRC Press, 2012.
[18] M. Kavehrad, Z. Zhou, M.S. Chowdhury, Short Range Optical Wireless: Theory and Applications, John Wiley & Sons, 2016.
[19] S. Rajagopal, et al., IEEE 802.15.7, TG7 Technical Considerations Document, 2015.
[20] S. Rajagopal, R.D. Roberts, S.-K. Lim, IEEE 802.15.7 visible light communication: modulation schemes and dimming support, IEEE Commun. Mag. 50 (3) (2012) 72–82, http://dx.doi.org/10.1109/MCOM.2012.6163585.
[21] M. Uysal, F. Miramirkhani, O. Narmanlioglu, T. Baykas, E. Panayirci, IEEE 802.15.7r1 reference channel models for visible light communications, IEEE Commun. Mag. 55 (1) (2017) 212–217, http://dx.doi.org/10.1109/MCOM.2017.1600872CM.
[22] B. Bai, Z. Xu, Y. Fan, Joint LED dimming and high capacity visible light communication by overlapping PPM, in: Proc. IEEE Annual Wireless and Opt. Commun. Conf., May, 2010, pp. 71–75, http://dx.doi.org/10.1109/WOCC.2010.5510410.
[23] M. Dyble, N. Narendran, A. Bierman, T. Klein, Impact of dimming white LEDs: chromaticity shifts due to different dimming methods, in: Proc. SPIE, vol. 5941, 2005, pp. 59411H, http://dx.doi.org/10.1117/12.625924.
[24] K. Lee, H. Park, Modulations for visible light communications with dimming control, IEEE Photon. Technol. Lett. 23 (16) (2011) 1136–1138, http://dx.doi.org/10.1109/LPT.2011.2157676.
[25] J.E. Gancarz, H. Elgala, T.D. Little, Overlapping PPM for band-limited visible light communication and dimming, J. Solid State Light. 2 (1) (2015) 3, http://dx.doi.org/10.1186/s40539-015-0022-0.
[26] S.H. Lee, S.-Y. Jung, J.K. Kwon, Modulation and coding for dimmable visible light communication, IEEE Commun. Mag. 53 (2) (2015) 136–143, http://dx.doi.org/10.1109/MCOM.2015.7045402.
[27] T. Komine, M. Nakagawa, Fundamental analysis for visible-light communication system using LED lights, IEEE Trans. Consumer Electron. 50 (1) (2004) 100–107, http://dx.doi.org/10.1109/TCE.2004.1277847.
[28] H. Park, J.R. Barry, Modulation analysis for wireless infrared communications, in: Proc. IEEE Intern. Conf. Commun. (ICC), vol. 2, IEEE, 1995, pp. 1182–1186, http://dx.doi.org/10.1109/ICC.1995.524287.
[29] J. Grubor, O. Jamett, J. Walewski, S. Randel, K.-D. Langer, High-speed wireless indoor communication via visible light, ITG Fachbericht (2007) 203–208.
[30] C.N. Georghiades, Some implications of TCM for optical direct-detection channels, IEEE Trans. Commun. 37 (5) (1989) 481–487, http://dx.doi.org/10.1109/26.24599.

[31] F. Cali, M. Conti, E. Gregori, IEEE 802.11 protocol: design and performance evaluation of an adaptive backoff mechanism, IEEE J. Sel. Areas Commun. 18 (9) (2000) 1774–1786, http://dx.doi.org/10.1109/49.872963.
[32] H. Takagi, L. Kleinrock, Throughput analysis for persistent CSMA systems, IEEE Trans. Commun. 33 (7) (1985) 627–638, http://dx.doi.org/10.1109/TCOM.1985.1096355.
[33] W. Zhang, S. Chowdhury, M. Kavehrad, Asynchronous indoor positioning system based on visible light communications, Opt. Eng. 53 (4) (2014) 1–10, http://dx.doi.org/10.1117/1.OE.53.4.045105.
[34] Z. Vatansever, M. Brandt-Pearce, Visible light positioning with diffusing lamps using an extended Kalman filter, in: Wireless Communications and Networking Conference (WCNC), 2017 IEEE, IEEE, 2017, pp. 1–6, http://dx.doi.org/10.1109/WCNC.2017.7925652.
[35] A. Chizari, M.V. Jamali, S. AbdollahRamezani, J.A. Salehi, A. Dargahi, Designing a dimmable OPPM-based VLC system under channel constraints, in: 2016 10th International Symposium on Communication Systems, Networks and Digital Signal Processing (CSNDSP), IEEE, 2016, pp. 1–6, http://dx.doi.org/10.1109/CSNDSP.2016.7573964.